Journal of Environmental Radioactivity 136 (2014) 22–29

Contents lists available at ScienceDirect

Journal of Environmental Radioactivity

journal homepage: www.elsevier.com/locate/jenvrad

Uranium(VI) remediation from aqueous environment using impregnated cellulose beads

Prashant Rule, Balasubramanian K*, Renuka R. Gonte

Department of Materials Engineering, Defence Institute of Advanced Technology (DU), Ministry of Defence, Girinagar, Pune 411025, India

ARTICLE INFO

Article history:
Received 26 November 2013
Received in revised form
11 April 2014
Accepted 5 May 2014
Available online 24 May 2014

Keywords:
Uranium
Impregnated cellulose
Adsorption
Kinetics

ABSTRACT

Use of cellulose based adsorbents for post treatment of contaminated water provides significant removal and recovery of trace quantities of radioactive and highly toxic U(VI) ions. Efficiency of the adsorbent was enhanced by impregnation of nano Fe_2O_3. Variables considered for obtaining optimized process conditions were solution pH, adsorbent dosage, initial metal ion concentration, additive content and contact time. The batch adsorption study revealed highly pH dependent adsorption with 100% adsorption efficiency at pH 7 using 1.5 g of adsorbent impregnated with 6 wt% Fe_2O_3 for 50 mL solution capacity in 150 min. The adsorption capacity was noted to be 7.6 mg/g. The adsorption mechanism was studied at pH 7 maintained using dilute ammonia solution to prevent the effect of any interfering cation. Uptake of U(VI) was found to be predominately via an intraparticle diffusion mechanism following pseudo second-order kinetic model, which is clearly reflected from the non-spontaneous thermodynamics yielding a positive free energy value. Recovery of the adsorbed U(VI) ions was highly feasible using 0.05 N HNO_3 and the regeneration of the adsorbent using 0.01 N NaOH.

1. Introduction

Serious concern regarding uranium contamination in ground water and soil has stemmed from its chemical toxicity, long half-life between 10^5 and 10^9 year and its use as a key element in the nuclear fuel cycle (Raskin and Ensley, 1999). Uranium is known to cause nephritis, a primary chemically induced effect causing inflammation of nephrons in the kidney, leading to kidney failure and death (Katsoyiannis, 2007; Harley et al., 1999). It is also considered as carcinogenic, causing bone cancer (Katsoyiannis, 2007). The main pathway of uranium ingression in the human body is through inhalation of dust and ingestion of contaminated water (Harley et al., 1999). Ground water contamination originates in the presence of bicarbonate ions which forms readily soluble uranyl complexes that are transported in the form of divalent uranyl ions or hexavalent carbonate complexes (Choy et al., 2006; Nishita et al., 1978). Literature reports the uranium exposure primarily through anthropogenic sources such as depleted mine tailings, medical wastes, by-products of weapon testing and nuclear power industry (Wild, 1993). The tolerable daily intake of uranium as established by WHO is 0.6 g/kg of body weight/day whereas the maximum uranium level in drinking water is 15 g/L (WHO, 2003, 2008). The maximum contaminant level (MCL) as set by USEPA for drinking water standard is 20 g/L (EPA, 2000). For example, the Safe Water Drinking Act of USEPA stipulates: "The uranium limit is 30 μg/L (micrograms per liter) in drinking water." (http://www.epa.gov/radiation/radionuclides/uranium.html).

Several techniques have been opted for removal and recovery of uranium from drinking water and industrial waste water. About 98% removal efficiency has been achieved using the ion-exchange method; however, it leads to generation of concentrated liquid wastes causing disposal issues (Camacho et al., 2010). Other techniques investigated include chemical clarification using ferric sulfate or aluminum sulfate, precipitation, membrane filtration, reverse osmosis, rhizofiltration, evaporation, etc. (Katsoyiannis, 2007; Mellah et al., 2007; Lozano et al., 1999; Agarwal et al., 2000; Oliver and Wilken, 1999; Kryvoruchko et al., 2004; Prasada Rao et al., 2006). These conventional methods however, involve high capital investment and maintenance cost; are ineffective at low concentration and generate highly contaminated waste products that require proper disposal. Adsorption has proven to be an effective and convenient technique amongst all the available methods due to its cost effectiveness, easy operation and wide choice of adsorbents (Ilaiyaraja et al., 2013).

Iron-based adsorbents are found to be useful for treatment of contaminated water due to their economic and safety virtues.

* Corresponding author.
E-mail addresses: meetkbs@gmail.com, balask@diat.ac.in (B. K).

http://dx.doi.org/10.1016/j.jenvrad.2014.05.004
0265-931X/

Literature reports the use of elemental iron(Fe^0) for removal of uranium ions from aqueous phase. Different mechanism for uranium removal such as precipitation, sorption and reduction has been proposed using elemental iron (Noubactep et al., 2006). Iron oxohydroxides have also demonstrated high sorption capacities for various metal contaminants (Waychunas et al., 2005). The iron oxyhydroxide phase akaganetite (−FeOOH) exhibits large tunnel-type structures which results in an interesting material for ion exchange (Yuan and Su, 2003). Application of zero valent iron nanoparticles for remediation of U-contaminated effluents revealed the uranium-Fe coupled redox mechanism and a highly effective and low-cost technology (Dickinson and Scott, 2010).

Impregnating nano Fe_2O_3 particles in the cellulose matrix provided additional advantages such as: (1) stability of the impregnated nanoparticles were enhanced due to prevention of aggregation and oxidation of Fe_2O_3; (2) adsorption capacity was enhanced due to presence of various functional groups such as acetate and hydroxyl functional groups of cellulose; additional due to the porosity of the impregnated matrix which provided huge surface area for adsorption; and (3) low-cost and is environmental-friendly adsorbent.

The primary objective of the present study was to investigate the various parameters having a potential impact on adsorption of U(VI) ions from aqueous solution using cellulose based adsorbent. This was achieved using nano Fe_2O_3 impregnated cellulose acetate beads under optimized experimental conditions in a batch adsorption process. The equilibrium isotherm, kinetic mechanism and thermodynamics of the adsorption process were studied at room temperature and fitted to various mathematical models to gain in-depth knowledge of the adsorption process.

2. Experiment section

2.1. Chemicals and materials

Cellulose acetate, dimethyl acetamide, acetone and uranium acetate were all purchased from Sigma Aldrich India. Hydrochloric acid, sodium hydroxide, glacial acetic acid and ammonia were obtained from Merck India. Deionized (DI) water was obtained from a Millipore Milli-Q system.

2.2. Synthesis of Fe_2O_3 impregnated cellulose beads

The hybrid adsorbents were synthesized according to our previously reported method (Ayalew et al., 2012; Gonte et al., in press-a,b). Briefly, requisite amounts of cellulose acetate, NaCl and Fe_2O_3 were dissolved in 1:2 acetone: dimethyl acetamide. The resulting mixture was precipitated in acid coagulation bath to yield uniform sized spherical beads. These hybrid beads were isolated and purified by washing with dilute NaOH followed by continuous water washing and finally dried to constant weight.

2.3. Batch sorption studies

A stock solution of U(VI) ions (100 mg/L) was prepared by dissolving the appropriate quantity of uranium acetate in deionized water and all the working solutions (25–100 mg/L) were prepared by further diluting the stock solution. Adsorption of uranium ions was evaluated by equilibrating optimized adsorbent dose in 100 mL uranium solution (100 mg/L) for 2 h at 400 rpm on an orbital shaker. Concentration of uranium in the supernatant solution was measured using a spectrophotometerically at 655 nm using Arsenazo(III) as a complexing agent (Savvin, 1961). The adsorption efficiency ($\%A_d$) and adsorption capacity (q) were calculated as

$$\%A_d = \left(\frac{(C_o - C_t)}{C_o}\right)*100 \quad (1)$$

$$q = \left(\frac{(C_o - C_t)}{w}\right)*V \quad (2)$$

where, C_o and C_t are the initial U(VI) ion conc. and U(VI) ion conc. at time t; w is weight of the adsorbent used (g) and V is the volume of the solution (L). The adsorption kinetics was studied by periodically evaluating the concentration of U(VI) ions in the supernatent solution.

3. Results and discussion

Uniform sized spherical Fe_2O_3 impregnated cellulose beads with an average diameter of 0.3 mm were obtained by precipitation polymerization technique. The resulting hybrid adsorbents revealed the presence of well defined flow lines and micro pores in the SEM micrographs (Fig. 1a,b), indicating the potential for capillary action. The surface porosity as calculated from the SEM images (ASTM B 276 standard, Gonte et al., 2012) was found to be 13.1%. The SEM micrographs of the adsorbent after uranium adsorption exhibited the presence of distinct surface rupturing and disappearance of flow lines (Fig. 1c,d).

3.1. Effect of parameters affecting adsorption

Effect of pH on sorption of U(VI) ions was monitored by changing the pH from pH 3–7 using 50 mg/L U(VI) ion conc. in 100 mL solution. pH of the solution was adjusted using dilute acetic acid and ammonium hydroxide at 25 °C. Inorganic acids and bases were not used so there would be no effect of interfering ions during sorption. Maximum sorption of 81% was achieved at pH 7 (Fig. 2a). Further increase in pH resulted in precipitation of U(VI) in the form of hydroxide whereas lowering the pH resulted in excess acetate ions in the solution which suppressed the U(VI) sorption.

Increasing the Fe_2O_3 content in the cellulose matrix from 0 to 100 wt% at pH 7 using 50 mg/L U(VI) ion conc. in 100 mL solution (Fig. 2b) resulted in increased adsorption due to the high affinity of Fe towards U(VI) ions. Reduced porosity and formation of highly compact beads was observed with increase in the Fe_2O_3 beyond 6 wt% which subsequently resulted in reduced adsorption. Cellulose acetate beads alone without impregnated nano Fe_2O_3 under identical conditions demonstrated only 10% removal efficiency whereas only nano Fe_2O_3 without the cellulose matrix revealed ~50% removal efficiency which was comparable to the 10 wt% Fe_2O_3 impregnated cellulose matrix. Nano Fe_2O_3 works under the mechanism of encapsulation and reduction of metal ions transforming it to less soluble, lower oxidation state.

For a fixed volume of solution (100 mL) and U(VI) ion concentration (50 mg/L) at pH 7, adsorption was found to increase with increase in sorbent dose from 0.5–0.7 g with no further enhanced adsorption beyond 0.7 g (Fig. 2c) which is due to the vacant active site.

Increase in initial U(VI) ion concentration from 25 mg/L to 100 mg/L (Fig. 2d) under optimized conditions (pH 7; bead dosage 0.7 g; Fe_2O_3 content 6 wt%) resulted in decreased adsorption from 81% to 57% however; the adsorption capacity increased from 1.7 mg/g to 7 mg/g. Increase in initial metal ion concentration results in increase in the adsorption capacity since it provides a driving force to overcome mass transfer resistances between the aqueous and solid phase. Decrease in sorption efficiency is due to limited number of active sites, which saturates beyond a certain

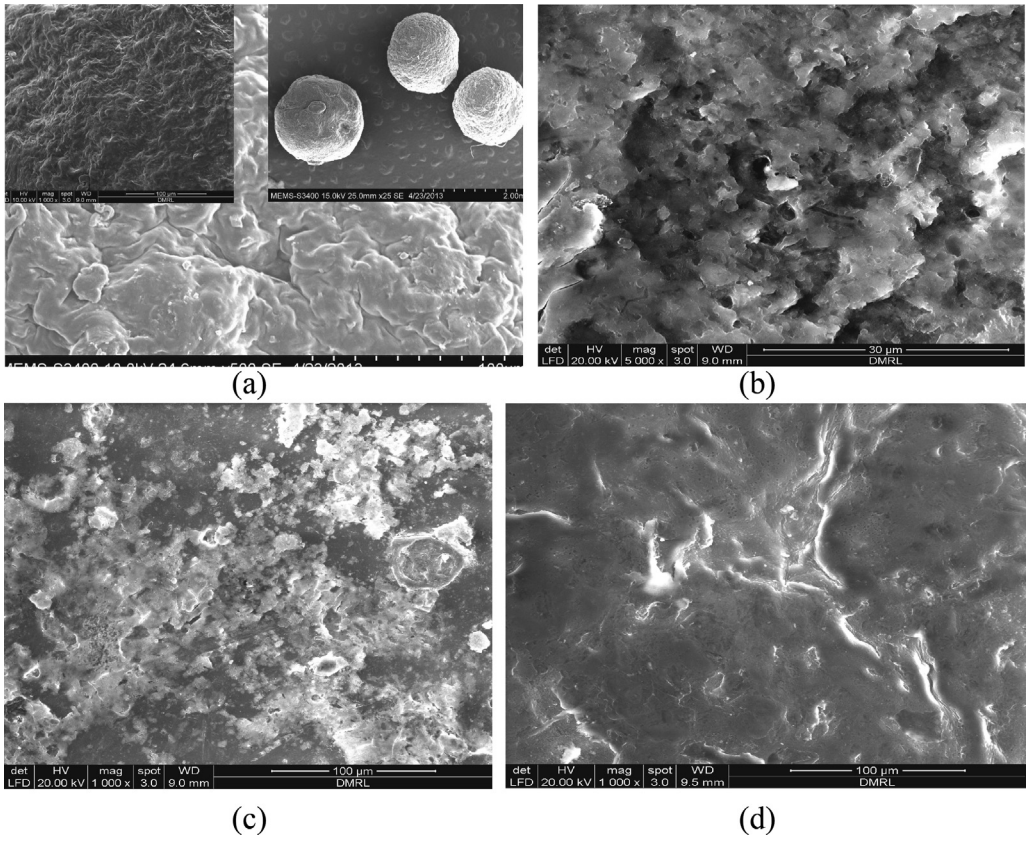

Fig. 1. SEM micrographs of Fe_2O_3 impregnated cellulose beads (a,b) before adsorption, and (c,d) after U(VI) adsorption.

concentration (Gonte and Balasubramanian, 2013; Gonte et al., in press-a,b).

3.2. Equilibrium adsorption isotherm

Adsorption isotherm studies are useful to determine the adsorption efficiency. These isotherms indicate the distribution of metal ion between the liquid phase and solid phase at equilibrium. Analysis of the isotherm data by fitting them to various isotherm models is an important step to find a suitable model for design purpose (Gonte and Balasubramanian, 2013; Gonte et al., in press-a,b).

3.2.1. Langmuir model

Langmuir model assumes a monomolecular layer formation when adsorption takes place without any interaction between the adsorbed molecules (Langmuir, 1916). The linearized Langmuir equation is:

$$C_e/q_e = (1/q_{\max} KL) + C_e/q_{\max} \quad (3)$$

where C_e is the equilibrium concentration (mg/L), q_e the amount of metal ion sorbed (mg/g), $q_{\max}$ is q_e for a complete monolayer (mg/g), and KL is a constant related to the affinity of the binding sites (L/mg).

A linear plot of C_e/q_e versus C_e with high regression coefficient value 0.992 (Fig. 3a) indicates the applicability of the model. The obtained equilibrium parameter $R_L = 0.3937$ indicates favorable adsorption.

3.2.2. Freundlich model

Freundlich isotherm is an empirical equation assuming adsorption on heterogeneous surfaces and relates the adsorption capacity with concentration of metal ions at equilibrium (Baudu et al., 2009). The linearized equation is:

$$\ln q_e = (1/n)\ln C_e + \ln K_F \quad (4)$$

where K_F and n are the Freundlich constants related to adsorption capacity and adsorption intensity respectively. A straight line plot of $\ln q_e$ versus $\ln C_e$ (Fig. 3b) yields the value of n to be 2.02 and R^2 value 0.9960 indicating highly favorable multilayered chemisorption.

3.2.3. Temkin model

The Temkin isotherm, considers that heat of adsorption decreases linearly with coverage and adsorbate–adsorbent interactions (Halsey, 1952). The Temkin equation is given as

$$q_e = (RT/b_T) \times \ln(a_T C_e) + (RT/b_T) \times \ln(C_e) \quad (5)$$

where R is gas constant 8.314×10^{-3} kJ mol^{-1} K^{-1}, T is absolute temperature K, b_T is the Temkin constant related to heat of adsorption (kJ mol^{-1}) and a_T is the equilibrium binding constant corresponding to the maximum binding energy (L/g).

The linear plot of q_e versus $\ln C_e$ (Fig. 3c) yields the constant b_T as 1.52 suggesting chemisorption and physisorption involved in the adsorption of the U(VI) ions.

3.2.4. D–R model

Dubinin (Bering et al., 1972) proposed an isotherm to estimate the mean free energy of adsorption. The linear form by equation:

$$\ln q_e = \ln q_{\max} - K\varepsilon^2 \quad (6)$$

where K (mol^2 kJ^2) is a constant related to the mean adsorption energy and ε is the Polanyi potential, calculated from equation:

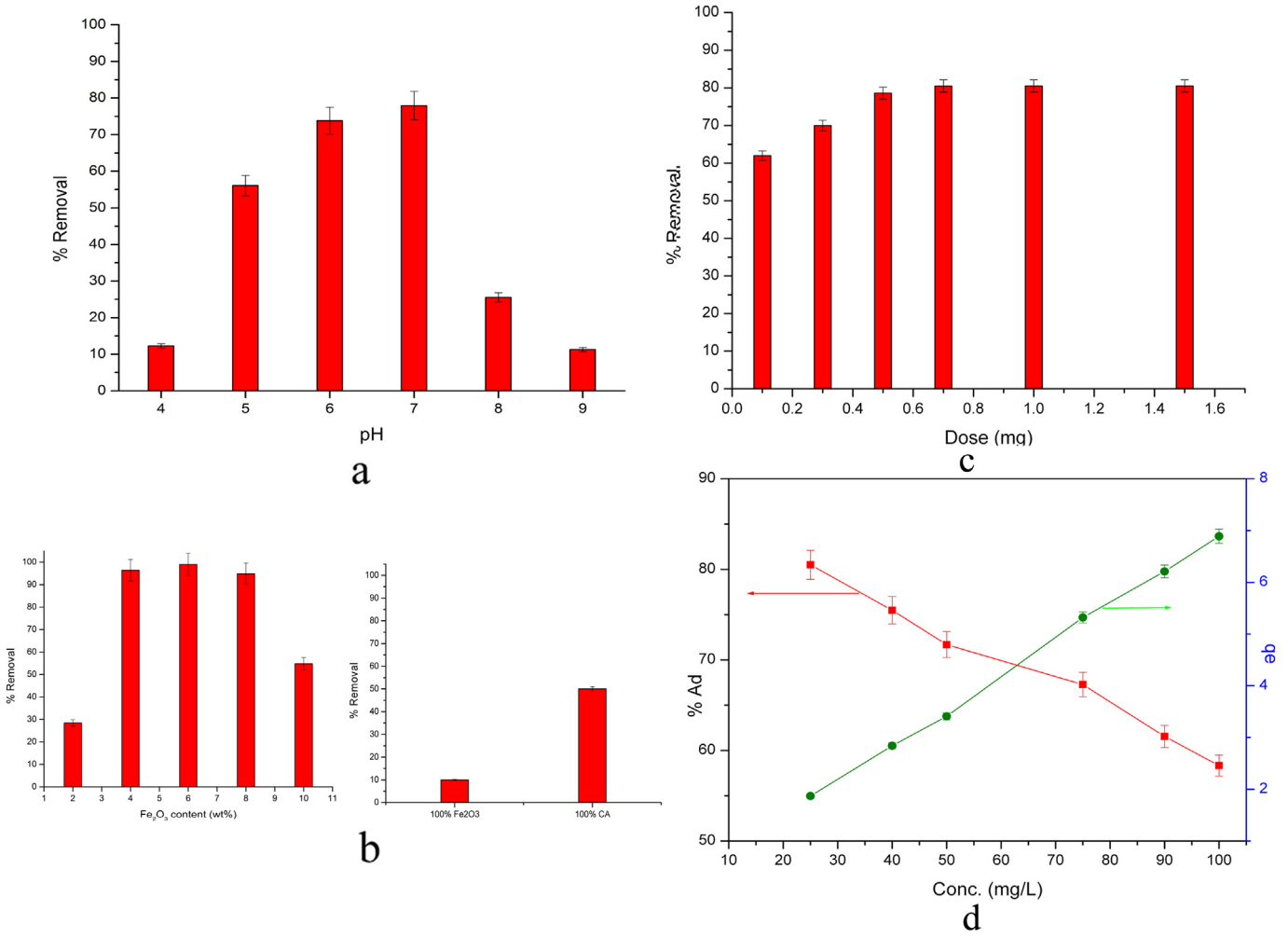

Fig. 2. Various parameters affecting adsorption (a) pH (b) Fe_2O_3 content (c) dose, and (d) initial U(VI) ion concentration.

$$\varepsilon = RT \ln(1 + (1/C_e)) \quad (7)$$

The plot between ln q_e and ε^2 (Fig. 3d) yields the constant K which is used to calculate the mean free energy E of sorption per molecule of the sorbate when it is transferred to the surface of the solid from infinity in the solution which is computed to be 0.3501 kJ/mol.

$$E = 1\Big/\sqrt{(2K)} \quad (8)$$

The various isotherm parameters are summarized in Table 1. The results are consistent with an hypothesis that the adsorption initiates as monolayer formation leading in multilayered chemisorption of U(VI) ion. The low energy associated with this adsorption is given by the D–R model.

3.3. Adsorption kinetics

The adsorption mechanism was investigated to determine the potential rate-controlling steps that include mass transport and chemical reaction process. Kinetic models have been exploited to analyze the experimental data to select the optimum condition for full scale batch process.

3.3.1. Pseudo first-order model

Lagergren showed that the rate of adsorption of solute on the adsorbent is based on the adsorption capacity and follows a pseudo first-order equation which is often used to estimate the "kad" considered as mass transfer coefficient in the design calculation. The pseudo first-order rate equation is given as:

$$\log(q_e - q_t) = \log q_e - (K_1/2.303) \times t \quad (9)$$

where q_e and q_t are the amounts of metal ion adsorbed at equilibrium and at time t respectively (mg/g), and K_1 is the first-order adsorption rate constant (min^{-1}). The straight line plot of log ($q_e - q_t$) vs. t (Fig. 4a) resulting in a negative slope and high regression coefficient value indicates good quality of linearization.

3.3.2. Pseudo second-order model

The pseudo second-order reaction is greatly influenced by the amount of metal ion on adsorbent's surface and at equilibrium. The rate is directly proportional to the number of active surface sites. The pseudo second-order equation is given as:

$$t/q_t = 1\Big/\left(K_2{*}q_e^2\right) + (1/q_e){*}t \quad (10)$$

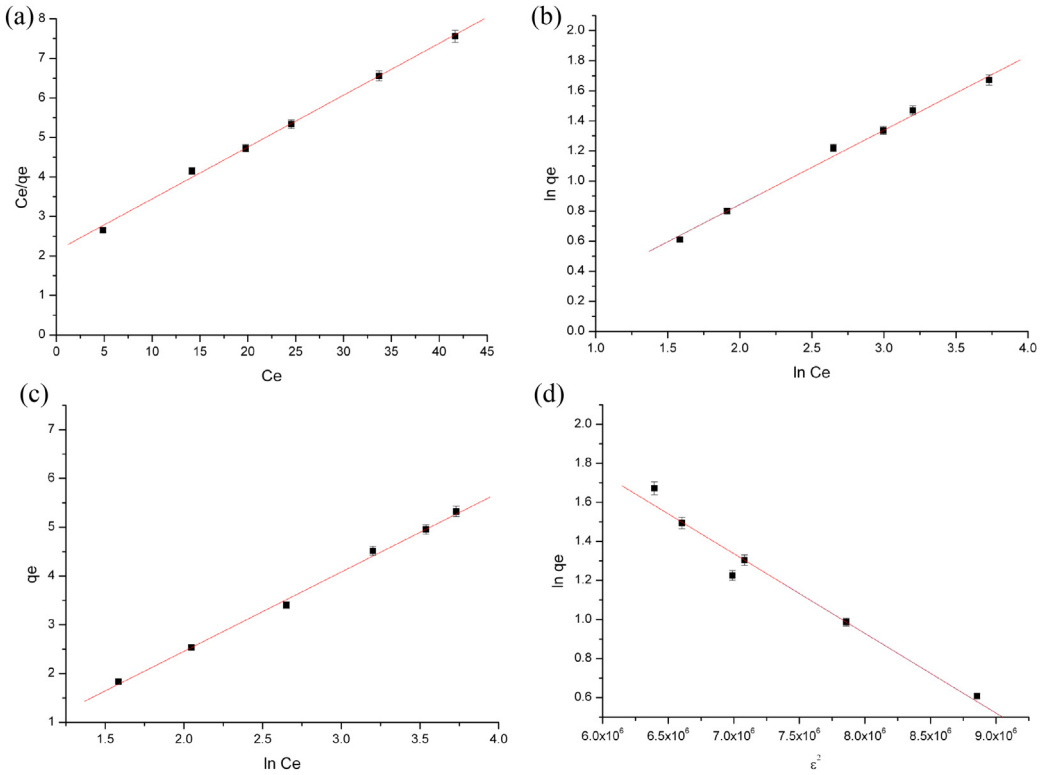

Fig. 3. Equilibrium isotherms models (a) Langmuir (b) Freundlich (c) Temkin, and (d) D–R.

where K_2 is the second order adsorption rate constant (g mg^{-1} min^{-1}), and q_e is the adsorption capacity calculated from the pseudo second-order kinetic model (mg/g).

The high regression coefficient constant (Fig. 4b) and nearly comparable q_e values suggests the sorption via pseudo second-order kinetic mechanism.

3.3.3. Elovich model

In reactions where the adsorbate molecules are chemisorbed on the solid surface of adsorbents without desorption, the rate of adsorption decreases with time due to increased surface coverage. Elovich model is the most useful model in describing 'activated' chemisorption. Elovich equation is a rate equation based on the adsorption capacity describing the adsorption on highly heterogeneous adsorbent. The linear form of the equation is given as

$$q_t = \ln\alpha\beta/\beta + \ln t\ /\beta \tag{11}$$

where α (mg g^{-1} min^{-1}) is the initial adsorption rate and β (g/mg) is the desorption constant related to the extent of surface coverage and activation energy for chemisorption. A straight line graph of q_t versus ln t yields (Fig. 4c) the slope and intercept which are used to calculate the kinetic constants. As mentioned in Table 2, the regression coefficients at all concentrations demonstrate good degree of linearization.

3.3.4. Intraparticle diffusion model

The rate-limiting step is an important factor governed by the adsorption mechanism. For a solid–liquid sorption process, the solute transfer is usually characterized by external mass transfer (boundary layer diffusion), or intraparticle diffusion, or both. The most commonly used technique for identifying the mechanism involved in the adsorption process is by fitting and intraparticle diffusion plot. The intraparticle diffusion coefficient is given as:

$$q_t = K_{\text{int}} \times t^{1/2} \tag{12}$$

where K_{int} is the intraparticle diffusion rate constant (mg g^{-1} min$^{-0.5}$). The plot of q_t versus $t^{1/2}$ presents multi-linearity with three step adsorption process (Fig. 4d) achieving equilibrium.

The various kinetic parameters are summarized in Table 2.

3.4. Thermodynamics of adsorption

Thermodynamic parameters such as free energy change, enthalpy and entropy of an adsorption were determined based on Van't Hoff plot. The data was obtained under optimized conditions as mentioned earlier. The q_e value was observed to be in the range 6–7 mg/g for the temperature range 20–35 °C which decreases with increase in temperature (~2.4 mg/g at 50 °C) suggesting the adsorption process is energy dependent mechanism (Fig. 5a). The steep and sudden decrease in q_e at 50 °C indicates that the weak Vander-waal's interaction, hydrogen bonding between uranyl ions

Table 1
Equilibrium isotherm constants.

Adsorption isotherm	Variables	
Langmuir	$q_{\max}$	7.6161
	K_L	6.1611×10^{-2}
	R_L	0.3937
	R^2	0.9920
Freundlich	n	2.0214
	K_F	0.8642
	R^2	0.9960
Temkin	b_T	1.5193
	R^2	0.9972
Dubinin–Radushkevich	$q_{\max}$	66.2013
	K	4.0799
	R^2	0.9616

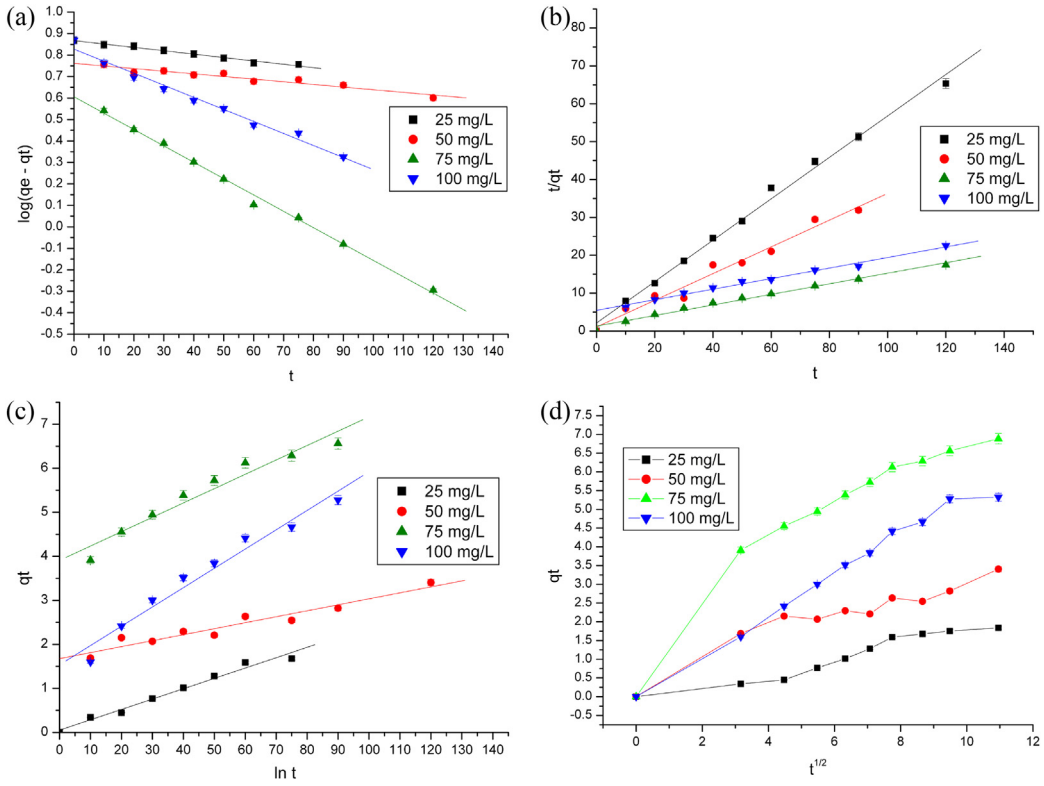

Fig. 4. Adsorption kinetic models (a) pseudo first-order (b) pseudo second-order (c) Elovich, and (d) Intraparticle diffusion.

and active sites of beads breaks at high temperature (Bayramoglu et al., 2006; Bhat et al., 2008).

The plot of ln K_d versus T^{-1} ((Fig. 5b) yielded the thermodynamic parameters such as enthalpy change (ΔH, in kJ mol^{-1}) and entropy (ΔS, in J mol^{-1} K^{-1}).

$$\ln K_d = (\Delta S/R) - (\Delta H/RT) \quad (13)$$

where K_d is the distribution coefficient

$$K_d = q_e/C_e \quad (14)$$

The change in Gibbs free energy was calculated from the equation

$$\Delta G = \Delta H - T\Delta S \quad (15)$$

where, R is the Universal gas constant = 8.314 J mol^{-1} K^{-1} and T is the absolute temperature (K).

The obtained values of ΔH and ΔS calculated from the plot of ln K_d versus $1/T$ are listed in Table 3. The negative ΔH and ΔS value suggests exothermic process with high degree of randomness in adsorption of uranium ions respectively. The positive values of ΔG indicates non-spontaneous adsorption of uranium ions. Increase in temperature from 298 K to 333 K results in increase the positive ΔG value further confirming the non-spontaneous adsorption.

3.5. Reutilization of adsorbed beads

Desorption of adsorbed uranium ions was found to be highly effective using 0.05 N HNO_3. It was observed that the adsorption efficiency of the beads decrease from 81% to 77% (Fig. 6) with repeated reuse of the sorbent for upto 5 cycles and desorption of uranium ions also decreased from 100% to 94%. The sorbent were activated using 0.01 N NaOH solution for repeated reuse.

4. Conclusions

The high adsorption efficiency of Fe_2O_3 impregnated cellulose beads was evaluated for uptake of U(VI) ions in a batch process. Rapid adsorption of trace quantity of U(VI) ions was achieved in 2 h. Adsorption was found to be highly pH dependent with maximum 81% adsorption at pH 7. Fe_2O_3 content in the beads also affected the sorption of U(VI) ions. Though nano Fe_2O_3 is itself used as a sorbent for metal ions, the main concept of impregnating Fe_2O_3 in cellulose acetate was to increase the adsorption capacity of cellulose acetate and improve the handling ability of Fe_2O_3. It was observed that the

Table 2
Adsorption kinetic parameters.

C_o (mg/L)	Pseudo first-order			Pseudosecond-order			Elovich model		
	Q_e	$K_1 \times 10^{-3}$	R^2	q_e	K_2	R^2	σ	Θ_σ	R^2
25	7.3739	3.6848	0.9829	1.8282	0.2606	0.9944	42.5532	1.5768	0.9807
50	5.781	2.7636	0.9253	2.8345	0.3371	0.973	73.5294	1.0081	0.9281
75	4.0365	17.5028	0.9956	7.1633	0.1078	0.9876	30.6748	1.0084	0.9456
100	6.7267	12.8968	0.9837	7.1685	0.0255	0.9894	22.8311	1.0289	0.9661

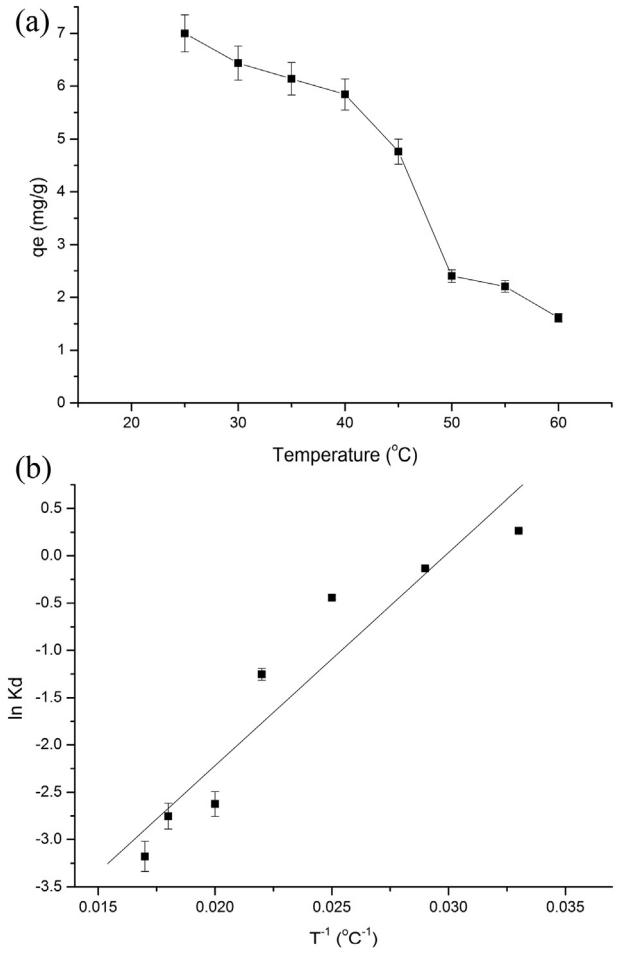

Fig. 5. Thermodynamics of adsorption (a) Temperature dependence of adsorption capacity (b) ln K_d versus T^{-1}.

Table 3
Thermodynamic parameters.

C_o (mg/L)	pH	ΔH (kJ/mol)	ΔS (J/(mol K))	ΔG (kJ/mol)				
				298 K	303 K	313 K	323 K	333 K
50	7	−1.87	−55.90	14.78	15.06	15.62	16.18	16.74

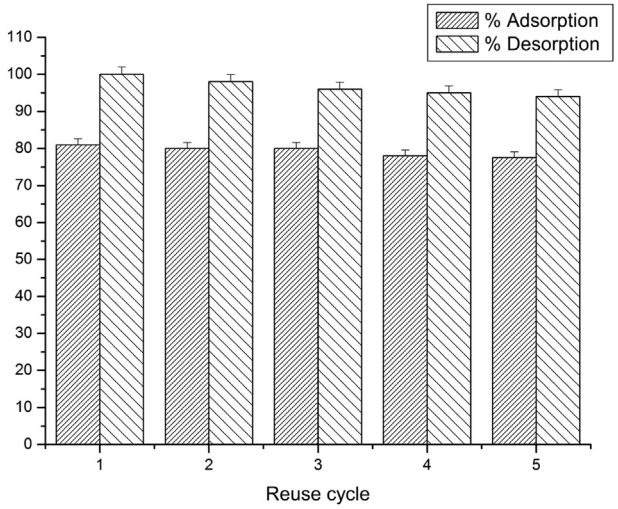

Fig. 6. Adsorption desorption cycles.

using only Fe_2O_3 as a sorbent yielded high adsorption capacity, however complete separation of U(VI) ion adsorbed Fe_2O_3 was a tedious process. Using such impregnated beads substantially minimized this problem since they could be separated by filtration process and also resulted in increased reusability and increased adsorption capacity.

The equilibrium parameters were consistent with sorption via monolayer formation further building into multilayer chemisorption with low sorption energy as indicated from the D–R model. The adsorption kinetics followed the pseudo second-order kinetic mechanism with good correlation between the experimental and theoretical q_e values and the intraparticle diffusion mechanism indicating the key role of the well-defined flow lines and pores observed on the adsorbent surface. The adsorption process was found to be exothermic and non-spontaneous process as indicated from the obtained thermodynamic parameters. The Fe_2O_3 impregnated cellulose beads demonstrated 5 effective reusable cycles with only 4% decrease in the adsorption efficiency. The regeneration of the beads was achieved by using 0.01 N NaOH solution for further use. These low cost adsorbents demonstrate high applicability for removal of uranium from drinking and industrial waste waters.

Acknowledgment

The authors thank Dr. Prahlada, Vice Chancellor, DIAT-DU for continuous encouragement and support. We are also grateful to Siddharth Dhumavat and Nitesh (VIT University) for technical assistance.

References

Agarwal, Y.K., Shrivatav, P., Mnom, S.K., 2000. Solvent extraction, separation of uranium(VI) with crown ether. Separation Purif. Technol. 20, 177–183.
Ayalew, A., Gonte, R.R., Balasubramanian, K., 2012. Development of polymer composite beads for dye adsorption. Int. J. Green. Nanotechnol. 4 (4), 440–454.
Baudu, B.M., Derriche, Z., Basly, J.P., 2009. Aqueous heavy metal removal on amine functionalized Si-MCM and Si-MCM-48. J. Hazard. Mater. 171, 1001–1008.
Bayramoglu, G., Celik, G., Arica, M.Y., 2006. Studies on accumulation of uranium by fungus *Lentnus sajor-caju*. J. Hazard. Mater. 136, 345–1345.
Bhat, S.V., Melo, J.S., Chaugule, B.B., D'Souza, S.F., 2008. Biosorption characteristics of uranium(VI) from aqueous medium onto *Catenella repens*, a red alga. J. Hazard. Mater. 158, 628–635.
Bering, B.P., Dubinin, M.M., Serpinsky, V.V., 1972. On thermodynamics of adsorption in micropores. J. Coll. Interf. Sci. 38, 185–194.
Camacho, L.M., Deng, S., Parra, R.R., 2010. Uranium removal from groundwater by natural clinoptilolite zeolite: effects of pH and initial feed concentration. J. Hazard. Mater. 175, 393–398.
Choy, C.C., Korfiatis, G.P., Meng, X., 2006. Removal of depleted uranium from contaminated soils. J. Hazard. Mater. 136, 53–60.
Dickinson, M., Scott, T.B., 2010. The application of zero-valent iron nanoparticles for the remediation of a uranium-contaminated waste effluent. J. Hazard. Mater. 178, 171–179.
EPA, 2000. Radionuclides Notice of Data Availability, Technical Support Document. USEPA Office of Groundwater and Drinking Water, 164 p.
Gonte, R.R., Balasubramanian, K., Deb, P.C., Singh, P., 2012. Synthesis and characterization of mesoporous hypercrosslinked poly(styrene co-maleic anhydride) microspheres. Int. J. Polym. Mater. 61, 919–930.
Gonte, R.R., Balasubramanian, K., Mumbrekar, J.D., 2013a. Porous and crosslinked cellulose beads for toxic metal ion removal – Hg(II) ions. J. Polym. (in press-a).
Gonte, R.R., Balasubramanian, K., 2013. Heavy and toxic metal uptake by mesoporous hypercrosslinked SMA beads: isotherms and kinetics. J. Saudi Chem. Soc. http://dx.doi.org/10.1016/j.jscs.2013.04.003.
Gonte, R.R., Shelar, G., Balasubramanian, K., 2013b. Polymer agro waste composites for removal of Congo red dye from waste waters: adsorption isotherms and kinetics. Desalin. Water Treat. http://dx.doi.org/10.1080/19443994.2013.833876.
Halsey, G.D., 1952. The role of surface heterogeneity in adsorption. Adv. Catal. 4, 259–269.
Harley, N.H., Foulkes, E.C., Hilborne, L.H., Hudson, A., Anthony, C.R., 1999. A Review of the Scientific Literature as it Pertains to Gulf War Illness, vol. 7. National Defense Research Institute MR-1018/7-OSD, Rand.
Ilaiyaraja, P., Deb, A.K.S., Sivasubramaniana, K., Ponrajub, D., Venkatramana, B., 2013. Adsorption of uranium from aqueous solution by PAMAM Dendron functionalized styrene divinylbenzene. J. Hazard. Mater. 250–251, 155–166.

Katsoyiannis, A., 2007. Carbonate effects and pH-dependence of uranium sorption onto bacteriogenic iron oxides: kinetic and equilibrium studies. J. Hazard. Mater. B139, 31–37.
Kryvoruchko, A.P., Yurlova, L.Y., Atamanenko, I.D., Kornilovich, B.Y., 2004. Ultrafiltration removal of U(VI) from contaminated water. Desalination 162, 229–236.
Langmuir, I., 1916. The constitution and fundamental properties of solids and liquids. J. Am. Chem. Soc. 38 (11), 2221–2295.
Lozano, J.C., Fernandez, F., Gomez, J.M.G., 1999. Preparation of alpha-spectrometric sources by co-precipitation with $Fe(OH)_3$: application to uranium. Appl. Radiat. Isotopes 50, 475–477.
Mellah, A., Chegrouche, S., Barkat, M., 2007. The precipitation of ammonium uranyl carbonates (AUC): thermodynamic and kinetics of investigation. Hydrometallurgy 85, 163–171.
Nishita, H., Wallace, A., Romney, E.M., 1978. Radionuclide Uptake by Plants. NUREG/CR0336. U.S. Nuclear Regulatory Commission, UCLA, pp. 12–1158.
Noubactep, C., Schoner, A., Meinrath, G., 2006. Mechanism of uranium removal from the aqueous solution by elemental iron. J. Hazard. Mater. B132, 202–212.
Oliver, R., Wilken, R.D., 1999. Removal of dissolved uranium by nanofiltration. Desalination 122, 147–150.
Prasada Rao, T., Metilda, P., Gladis, J.M., 2006. Preconcentration technique for uranium(VI) and uranium(IV) prior to analytical determination. Talanta 68, 1047–1064.
Raskin, I., Ensley, B.D., 1999. Phytoremediation Toxic Metals Using Plants to Clean Up the Environment. John Willey & Sons, ISBN 978-0-471-19254-1, 304 p.
Savvin, S.B., 1961. Analytical use of arsenazo(III), determination of thorium, zirconium, uranium and rare earth elements. Talanta 8, 673–685.
Waychunas, G.A., Kim, C.S., Banfield, J.F., 2005. Nanoparticulate iron oxide minerals in soils and sediments: unique properties and contaminant scavenging mechanisms. J. Nanopart. Res. 7, 409–433.
WHO, 2003. Guidelines for Drinking Water Quality, third ed.
Wild, A., 1993. Soils and the Environment: an Introduction. Cambridge University Press, ISBN 9780511623530. http://dx.doi.org/10.1017/CBO9780511623530.
World Health Organization, 2008. Guidelines for Drinking Water Quality. In: Incorporating the First and Second Addenda, Recommendations, Geneva, third ed., vol. 1 515 p.
Yuan, Z.Y., Su, 2003. Surfactant-assisted nanoparticle assembly of mesoporous-FeOOH (akaganeite). Chem. Phys. Lett. 381, 710–714.